Journal of The Electrochemical Society, **153** (5) C325-C331 (2006)
0013-4651/2006/153(5)/C325/7/$20.00 © The Electrochemical Society

Electrodeposition of Ni from Low-Temperature Sulfamate Electrolytes

II. Properties and Structure of Electrodeposits

S. H. Goods,[a,z] J. J. Kelly,[b,*] A. A. Talin,[a] J. R. Michael,[c] and R. M. Watson[a]

[a]*Sandia National Laboratories, Livermore, California 94551, USA*
[b]*IBM, T.J. Watson Research Center, Yorktown Heights, New York 10598, USA*
[c]*Sandia National Laboratories, Albuquerque, New Mexico 87185, USA*

The structure and properties of Ni deposited from sulfamate electrolytes is reported. Particulate filtering of the electrolyte has significant consequences with respect to the microstructure and resulting mechanical properties. Effects were most pronounced at low current densities, and gradually disappeared as current density increased. At low current density (3 mA/cm^2), deposits plated from a filtered electrolyte were fine-grained and exhibited ⟨011⟩ texture orientation, characteristic of "inhibited" growth. The strengths of these deposits ranged from 700 MPa to 1 GPa; increasing with increasing deposition temperature from 28 to 50°C. Low-current-density deposits from unfiltered electrolyte exhibited a temperature dependent instability in grain morphology and texture. At low temperatures (≤32°C) deposits were coarse grained and predominantly ⟨001⟩, while at 50°C, deposits were fine grained and ⟨011⟩. At intermediate temperatures, the deposits grew initially in the uninhibited, coarse grain ⟨001⟩ mode but then transitioned to the fine grain, ⟨011⟩ inhibited growth mode. At high current density (15 mA/cm^2), the structure and properties of electrodeposits were unaffected by particle filtering. Irrespective of deposition temperature or filtering condition, deposits had the grain morphology and crystallography characteristics of uninhibited growth – namely, coarse, columnar grains with preferred ⟨001⟩ texture. The measured strength of these deposits were 350–400 MPa.
 [DOI: 10.1149/1.2181447]

Manuscript submitted October 6, 2005; revised manuscript received January 6, 2006. Available electronically March 27, 2006.

Electrodeposition of nickel from sulfamate electrolytes has found wide use in many commercial and industrial applications,[1-8] and the rational for its use was described in Part I of this work. More recently, electrodeposited nickel from sulfamate (hereafter referred to as ED Ni-sulfamate) has become a favored material for the electrodeposition of microsystem components using the LIGA process (an acronym for the German words for: lithography, electroplating, and molding). While the LIGA process was introduced in Part I, since the test specimens studied in this second part were fabricated using the LIGA process, we describe it here in greater detail.

Briefly, a thick (100s to 1000s of micrometers) polymer photoresist blank, bonded to a metallized substrate (viz., the plating base), is lithographically patterned using a synchrotron X-ray source and developed to yield a mold consisting of deep prismatic cavities having feature sizes measuring in the 10s to 100s of micrometers. It is into these cavities that an elemental metal or alloy is electrodeposited. As these microcomponents may perform mechanical functions, their microstructure and mechanical properties are of interest, as well as the deposition conditions that may affect them. As stated in Part I, while the process–structure–property relationships are generally known for ED Ni-sulfamate under typical operating conditions,[9,10] the successful integration of the electrodeposition step with other steps in the LIGA process may necessitate deposition conditions that differ from standard plating practice.

In particular, it may be necessary to operate plating cells at temperatures well below those recommended by common practice in order to reduce thermal distortions of the resist material that define the lateral dimensions of a structure.[11] Another aspect that must be considered for the successful integration of the electrodeposition step into the LIGA process is the deposition current density. Transport limitations, particularly important in narrow, high-aspect-ratio features where circulation of the bulk electrolyte is impeded, are typically minimized by reducing deposition rates. This is most straightforwardly done by depositing metal at low current densities. In the first part of this work, we reported the electrochemistry and process dependence of the intrinsic film stresses of ED Ni-sulfamate over a range of current densities and bath temperatures. In this second part, the effects of these conditions on the mechanical properties and microstructure of net shape material plated using the LIGA process are presented.

* Electrochemical Society Active Member.
z E-mail: shgoods@sandia.gov

Experimental

Deposition.— The composition of the Ni-sulfamate electrolyte is the same as that presented in Part I: 1.35 M $Ni(SO_3NH_2)_2$, 30 g/L boric acid, and 0.2 g/L sodium dodecyl sulfate (as a wetting agent that reduces pitting and otherwise has no effect on the Ni).[12] The deposition parameters for net shape fabrication of test specimens and structures are within the same range of those used for film stress measurements in Part I. In this work, the influence of deposition temperature was examined at 28, 32 (the minimum manufacturer recommended deposition temperature), 40, and 50°C. A pH of 3.5 ± 0.1 was used for all deposition runs; the typically recommended range is from 3.5 to 4.5. Details related to the preparation of the Ni anodes and the as-received sulfamate electrolyte are described in Part I as well. In particular, we note here that new baths that were purified by a carbon treatment before their initial use and wound, 5-μm polypropylene fiber filters (Floking) were used as the particle and debris collecting media.

Mechanical testing.— Net shape tensile specimens were fabricated using the LIGA process as described above. Tensile specimens had a reduced gauge section measuring 0.76 × 0.25 mm (width × thickness) and an overall gauge length of 6.2 mm. After final planarization and release from the substrate, the mechanical test specimens were tested in uniaxial tension in an Instron model 5848 microtester. Load was measured using a 1-kN load cell and displacement was measured using a noncontacting laser extensometer (EIR model LE-01) having approximately 1-μm resolution. Tests were performed at room temperature at a constant extension rate of 5×10^{-4} mm/s.

Microscopy.— A FEI DB235 dual beam focused ion beam (FIB) scanning electron microscope (SEM) was used to characterize the microstructure of as-deposited samples employing the ion beam-induced channeling contrast imaging (ICI) capabilities of the FIB instrument.[13] The depth of penetration of the ions is related to the crystallographic orientation of individual grains. As such, certain crystallographic orientations result in stronger ion channeling and therefore deeper penetration of the ions into the sample. Deeper ion

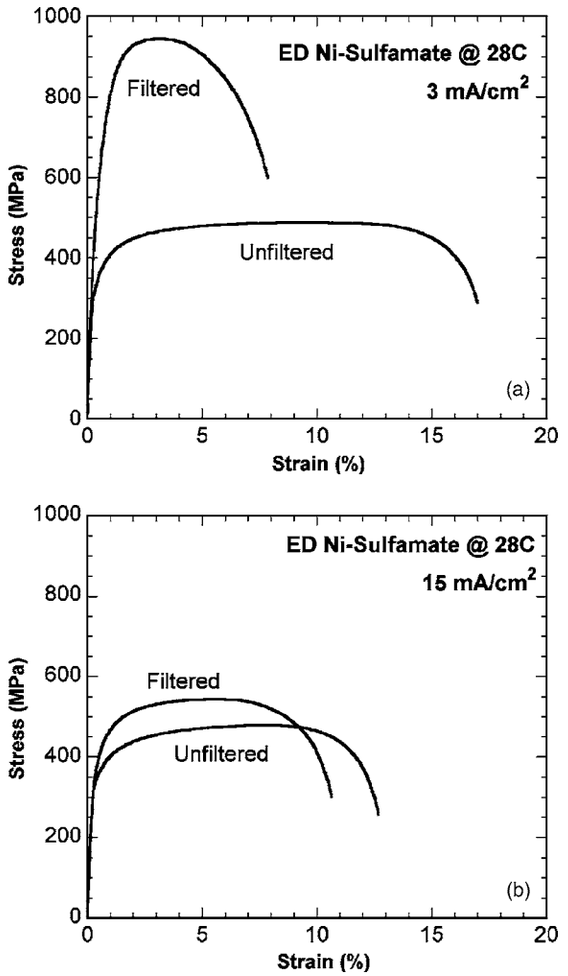

Figure 1. Tensile behavior of electrodeposited nickel from sulfamate electrolytes at 28°C. (a) High strength is observed in low current density deposits fabricated from particle filtered electrolyte. (b) Filtration has little effect on mechanical properties when deposition occurs at higher current density.

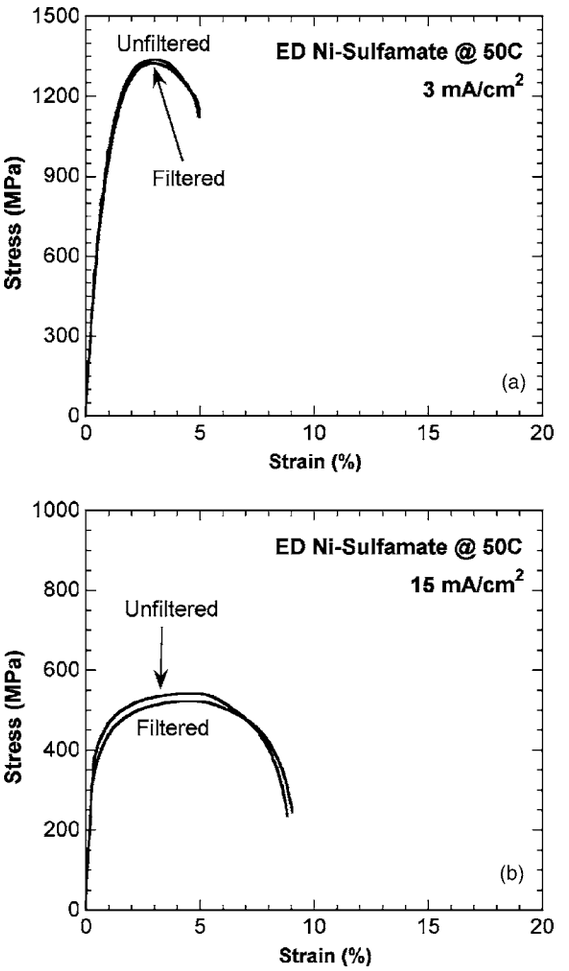

Figure 2. Tensile behavior of electrodeposited nickel from sulfamate electrolytes at 50°C. (a) High strength is observed in low current density deposits independent of filtering condition. (b) Much lower strength is observed in high current density deposits independent of filtering condition.

penetration, in turn, produces fewer collectable secondary electrons, so strongly channeling orientations appear dark as compared to more weakly channeling orientations. The amount of channeling is quite sensitive to small variations (1–2°) in orientation so that not only can grains of different orientations be imaged, but small misorientations within a grain can be visualized as well.

Electron backscatter diffraction (EBSD), performed on a Zeiss Supra 55VP field emission gun SEM using an HKL Technology camera and Channel 5 software, was used to map the through-thickness grain orientation (texture) from metallographically prepared cross sections of the as-deposited test specimens.

X-ray characterization.— Specimen texture was determined using a Philips X'Pert MRD X-ray diffractometer with a Cu anode operated at 45 kV and 40 mA. Pole figures corresponding to (111), (200), and (220) reflections were collected for azimuthal rotation of $0 \leqslant \phi \leqslant 360°$ and tilt angle of $0 \leqslant \psi \leqslant 90°$ in 5° increments. The experimental pole figures were corrected for absorption and defocusing using a Ni powder specimen.[14] Based on the experimental pole figures (data for only $\psi \leqslant 80°$ was used), orientation distribution functions (ODFs) were computed using the BEARTEX program;[15] the ODFs were in turn used for calculation of inverse pole figures.

Results and Discussion

Filtering effects on mechanical properties.— In Part I of this work, it was shown that the most pronounced effect of filtering on blanket film stress occurred at low current densities and low plating temperature. Not surprisingly, the as-plated mechanical properties parallel this effect. Figure 1a and b illustrates the typical tensile behavior for electrodeposited test specimens, all plated at 28°C and at the current densities and filtering conditions indicated. Stress-strain curves for the material deposited at 3 mA/cm^2 are shown in Fig. 1a. For each filtering condition, the tensile behavior is quite reproducible. Material deposited from an unfiltered bath exhibit yield and ultimate tensile strengths of 350 and 500 MPa, respectively, similar to the values reported for nickel deposits from a sulfamate bath in the literature.[16,17] It is clear from Fig. 1a that particle filtering has a significant effect on both the yield and ultimate tensile strength (UTS), with each increasing to 730 and 950 MPa, respectively.

Conversely, particle filtering has little effect on the mechanical properties of the electrodeposits when plated at a current density of 15 mA/cm^2 as illustrated in Fig. 1b, where tensile curves are presented for each filtering condition. It is evident that, at this higher current density, filtering induces only a small increase in the yield and UTS: 360 and 475 MPa (yield strength) for the material deposited from an unfiltered bath vs 410 and 540 (UTS) MPa for the

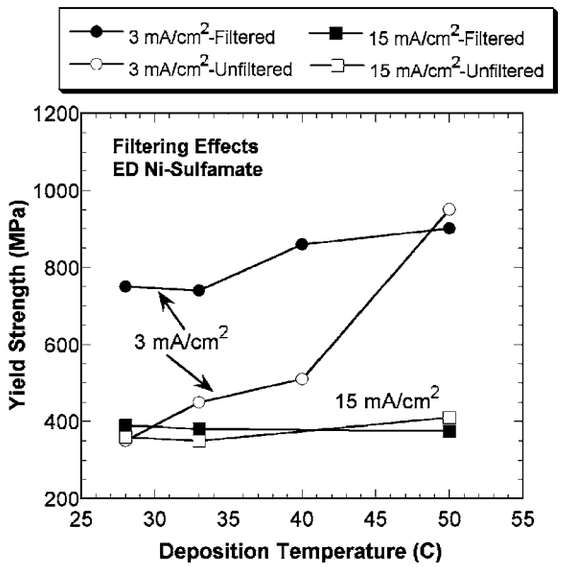

Figure 3. Summary of process parameter effects on strength (average of 3–4 tensile tests) of electrodeposited nickel from sulfamate electrolytes. High-current-density deposits always exhibit low strength. Low-current-density deposits from filtered electrolyte always exhibit high strength. Low-current-density deposits from unfiltered electrolyte exhibit monotonically increasing strength as deposition temperature increases.

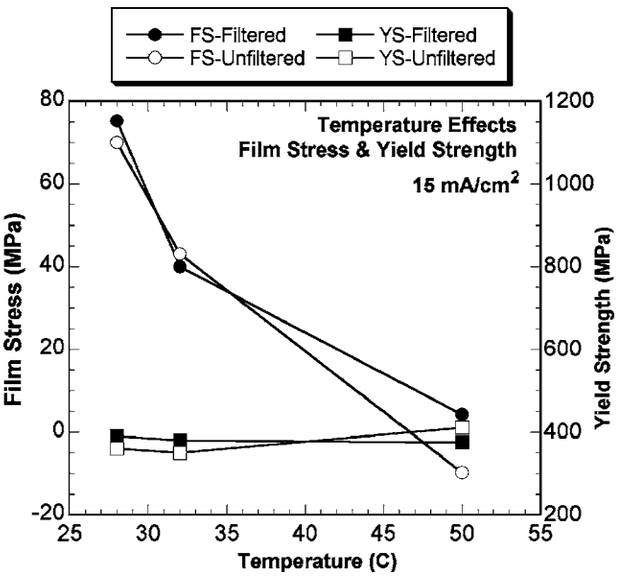

Figure 4. Comparison of intrinsic film strength (FS) and electrodeposit yield strength (YS) for ED Ni–sulfamate deposited at 50°C. Film stress and strength of electrodeposits do not correlate.

material plated from a filtered bath. It is also clear from comparing Fig. 1a and b that current density plays no role in determining mechanical properties in unfiltered baths, both baths yielding material with virtually the same mechanical properties.

Figure 2a and b illustrates the typical tensile behavior for specimens deposited at the highest temperature, 50°C. For specimens deposited at the lowest current density, 3 mA/cm^2, the presence or absence of filter has no effect on the mechanical properties. Indeed, the tensile curve for filtered and unfiltered specimens are essentially indistinguishable from each other. However, these deposits have extremely high strength (note the scale change on the strength axis), as high or higher than that reported in previous literature.[9,16,17] For specimens deposited at 15 mA/cm^2, filtering (or its absence) again has no measurable effect on properties, but in this instance strength was low and comparable to that of the specimens deposited at 28°C and at the same current density, 15 mA/cm^2.

Figure 3 and Table I summarize the strength measurements for specimens deposited at all temperatures, current densities, and bath filtering conditions. Both indicated average strength values (yield and UTS) from 3–4 individual tensile tests. It is evident from Fig. 3 that the mechanical properties of ED Ni–sulfamate are insensitive to the presence or absence of particle filtration when plated at the high current density over the entire temperature range examined. For these 15-mA/cm^2 specimens, yield strength is universally low and ranges from about 350 MPa to no higher than 410 MPa. At the low current density, however, specimens plating in unfiltered cells show a progressive increase in strength as the plating temperature increases. For these specimens, yield strength ranged from 350 MPa at 28°C to 950 MPa at 50°C. Lastly, the specimens deposited at the low current density from the filtered cells show universally high strength, with some indication that the strength increases with increasing deposition temperature. In this instance, the yield strength increased from 750 MPa (at 28°C) to 900 MPa (at 50°C).

Figure 4 compares the intrinsic film stress results from Part I of this work to the current yield strength measurements for ED Ni–sulfamate deposited at 15 mA/cm^2. The previous film stress measurements revealed relatively high stresses (70–75 MPa) for films deposited at the lowest temperature. Figure 4 shows that these film stresses decrease monotonically with increasing deposition temperature for both the filtered and unfiltered electrolyte, so that at a deposition temperature of 50°C the film stresses are quite low. In contrast, the yield strengths of the deposits are low for all deposition temperatures and filtering conditions. It is evident that there is no correlation between the intrinsic film stress of these deposits and the resultant mechanical properties. Similarly, for other plating conditions (temperature and filtering condition), there is no correlation between the deposit film stress and the strength of the deposited material.

Table I. Deposition parameter effects on average mechanical properties.

Temperature (C)	Current density (mA/cm^2)	Filtered		Unfiltered	
		YS	UTS	YS	UTS
28	3	750	925	350	490
	15	390	550	360	470
32	3	740	980	450	660
	15	380	500	350	490
40	3	860	1205	505	720
50	3	900	1340	950	1350
	15	375	525	410	540

Filtering effects on microstructure.— Figure 5a shows an ICI of a cross section for a specimen plated at 3 mA/cm^2 from an unfiltered electrolyte where the plating direction is from the bottom of the image to the top. The coarse, columnar microstructure is typical of ED Ni–sulfamate plated under conditions where deposition is said to be "uninhibited."[18] We note that the microstructure revealed in this figure is characteristic of the electrodeposits plated from both 15 mA/cm^2 plating cells as well, and for the sake of brevity those micrographs are not shown. The very bottom of the image includes the initial deposition of nickel upon the metallized LIGA mold substrate. The grain size is initially extremely fine over the first micrometer or two, but evolves rapidly to the much coarser grain structure that is characteristic of the bulk deposit. This initiation zone where grain size and structure evolve rapidly is commonly observed in electrodeposits.[5] Figure 5b shows an EBSD map of this deposit in

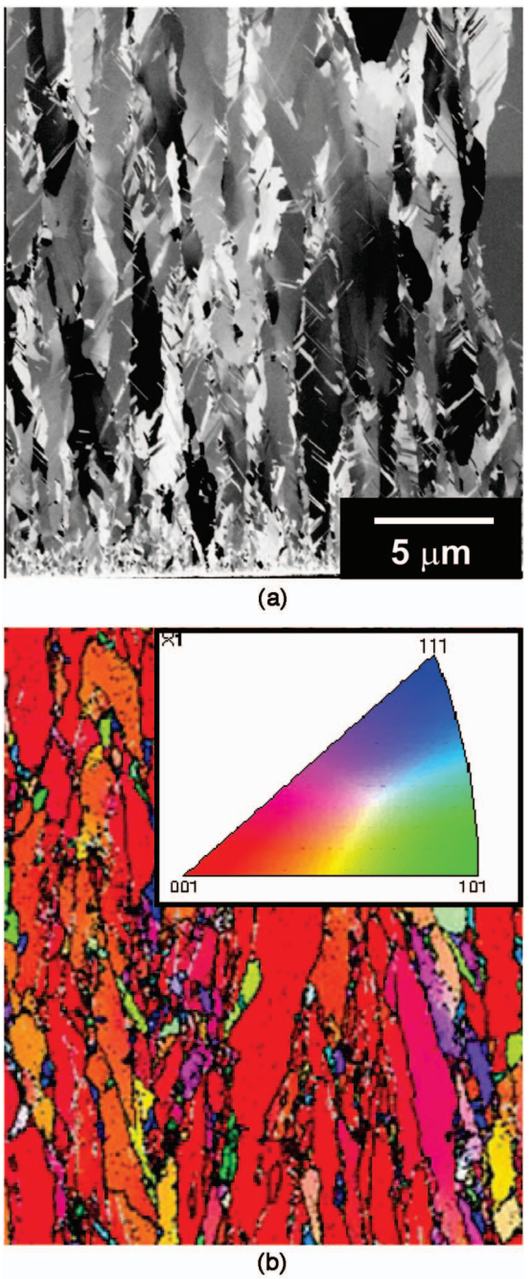

Figure 5. (Color) (a) ICI micrograph of electrodeposit cross section from specimen deposited at 28°C, 3 mA/cm^2 in unfiltered electrolyte. Deposition direction is vertical and a finer grain initiation zone is seen at the bottom of the micrograph. (b) EBSD map indicates that the microstructure is predominantly ⟨001⟩. The coarse-grain ⟨001⟩-textured microstructure is indicative of uninhibited growth. Specimens from the 15-mA/cm^2 deposits at this temperature exhibited similar grain size and texture.

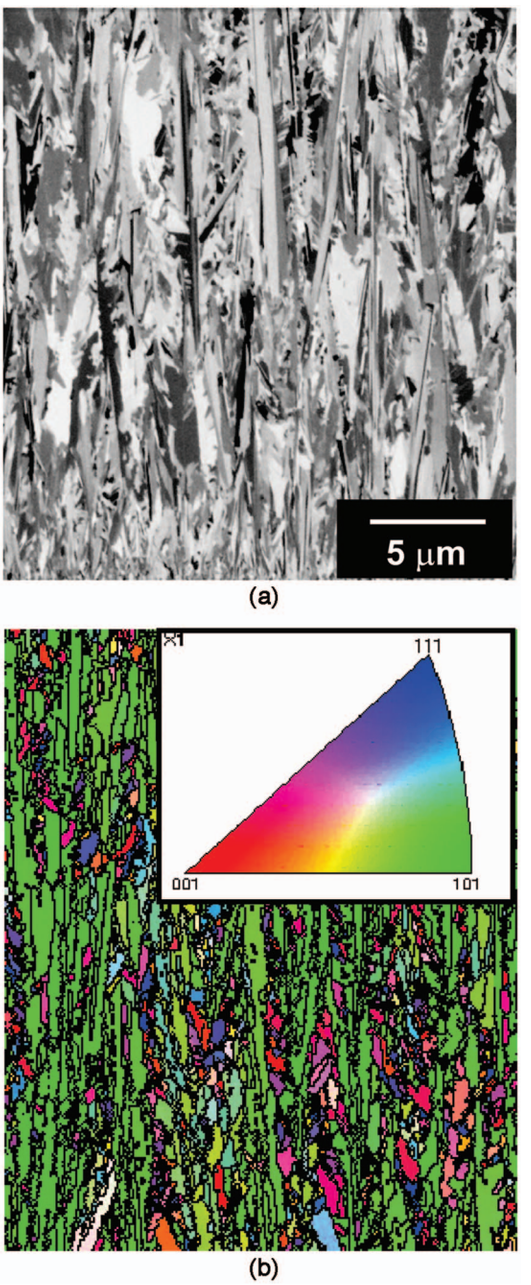

Figure 6. (Color) (a) ICI micrograph of electrodeposit cross section from specimen deposited at 28°C, 3 mA/cm^2 in filtered electrolyte. Deposition direction is vertical and the initiation zone of the deposit is seen at the bottom of the micrograph. (b) EBSD map indicates that the microstructure is predominantly ⟨011⟩. The fine grain size and ⟨001⟩-textured microstructure is indicative of inhibited growth.

cross section (except for the initiation zone). The false color inset is an inverse pole figure (IPF) schematic and indicates that the deposit exhibits a high degree of texture (here texture is referenced to the growth direction normal, that is, the "out-of-plane" texture).[d] The inset legend reveals that the texture is predominantly ⟨001⟩, which is also indicative of "uninhibited" growth for ED Ni. Additional texture mapping indicated that all deposits had a fiber texture, typical of thick EDs.

Figure 6a shows a similar ICI image of the cross section of a specimen plated at 3 mA/cm^2 in a filtered electrolyte. We note that the initiation zone is still apparent at the bottom of the micrograph but it is evident that the columnar grain size in the bulk is much finer than in the previous instance. This finer grain size is responsible for the considerably higher yield strength[19] of the deposit as shown in

[d]The EBSD image in Fig. 5 and subsequent figures are not purported to be of the precise region shown in the ICI images, as both images are obtained from different microscopes requiring intermediate surface preparation. Rather, the EBSD images are taken from the same surfaces as represented by the companion grayscale ICI image.

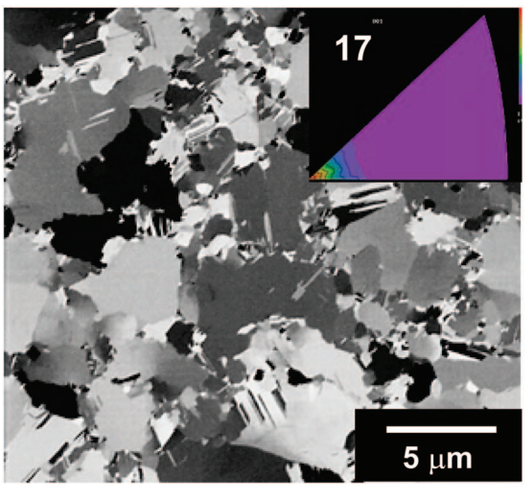

Figure 7. (Color) Planview image of deposit shown in Fig. 5. XRD-generated IPF inset indicates that the ⟨001⟩ texture is 17 times random.

Fig. 1 and 3 and is characteristic of inhibited film growth. Inhibited growth in electrodeposits results not only in finer grain size material, but also in a change in the characteristic texture from ⟨001⟩ to ⟨011 ⟩. Indeed, the EBSD-derived map shown in Fig. 6b confirms this change in out-of-plane texture to ⟨011⟩.

Figure 7 shows a planview orientation of the same deposit shown in Fig. 5a. Line intercept analysis performed on this SEM image indicated that the average grain size for this electrodeposit was approximately 1.0 μm. The inset in Fig. 7 is an X-ray diffraction (XRD)-generated IPF that confirms that the preferred texture is ⟨001⟩. Since XRD samples a larger planar area of the deposit than is the case for EBSD, the degree of preferential texture can be assessed more quantitatively. For this deposit, the texture is ~17 times random, indicating a high degree of texture. Figure 8 shows a similar planview image for a specimen plated under conditions as for the specimen shown in Fig. 6a. Line intercept analysis performed on this SEM image indicates that the average grain size for this electrodeposit is nearly five-fold smaller than for the electrodeposit shown in the previous figure, ~200 nm. The IPF inset in Fig. 8 confirms the EBSD texture analysis as being ⟨011⟩, and the degree

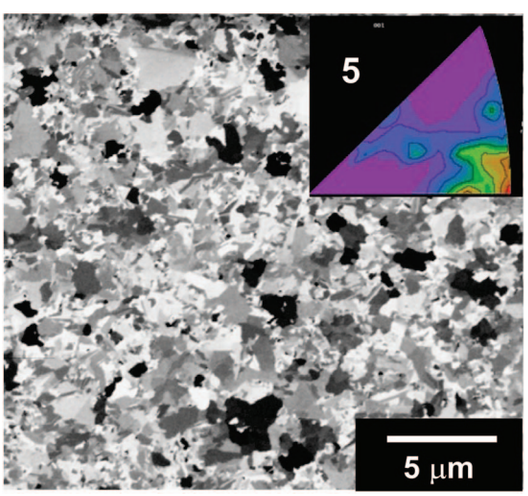

Figure 8. (Color) Planview image of deposit shown in Fig. 6. XRD-generated IPF inset indicates that the ⟨011⟩ texture is approximately 5 times random.

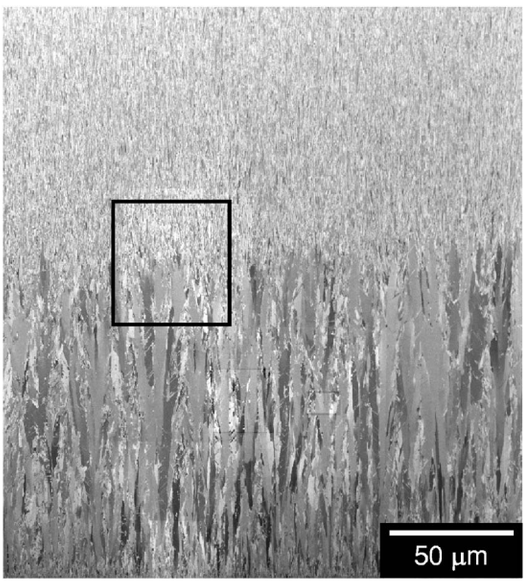

Figure 9. ICI micrograph of electrodeposit cross section from specimen deposited at 40°C, 3 mA/cm^2 in unfiltered electrolyte. The micrograph in the vertical direction spans the entire thickness of the deposit. The deposit is initially coarse-grained but abruptly transitions to a fine-grain size. The windowed region is shown at higher magnification in Fig. 10.

of texturing in this instance was 5 times random. The IPF also gives an indication there is a small amount of texturing associated with higher index directions.

The microstructure of the electrodeposits plated at 50°C and 15 mA/cm^2 in both filtered and unfiltered electrolyte exhibit the same characteristics as that shown in Fig. 5 and 7, that is, coarse-grained and ⟨001⟩-textured, characteristic of an uninhibited growth mode for Ni. The only difference observed at 50°C (derived from the filtering condition) is a greater degree of preferred orientation for deposit plated from unfiltered electrolyte, 50 times random, vs 16 times random for the deposit from filtered electrolyte. The coarse grain structure of both of these deposits is reflected in their low yield strength, as shown in Fig. 3. The 50°C deposits plated at 3 mA/cm^2 have very high yield strengths and not surprisingly exhibit a fine grain size and ⟨011⟩ texture very similar to that shown in Fig. 6 and 8. XRD-derived texture revealed that, for the filtered deposit, the ⟨011⟩ texture was 7 times random while for the unfiltered deposit it was 15 times random.

Figure 3 shows that the electrodeposit plated at 40°C and at 3 mA/cm^2 from an unfiltered electrolyte exhibits a yield strength that is intermediate between that of the high current density deposits and that of the low current density deposit from the filtered electrolyte. It is reasonable, therefore, to imagine that the microstructure of the deposit would consist of a mixture of the both the coarse-grained, ⟨001⟩-textured material and the fine-grained, ⟨011⟩-textured material. Figure 9 shows that this is indeed the case. Here, as in earlier figures, the growth direction is from the bottom to the top of the image. Rather than a uniform mixture of fine- and coarse-grained material, leading to the increased strength, Fig. 9 reveals the deposit to be duplex in nature, consisting of an initially coarse-grain columnar structure (disregarding the initiation zone at the very bottom of the micrograph) which abruptly transitions to a fine-grained structure at a point very near the mid-thickness of the deposit. Figure 10a shows a higher magnification image of the region outlined in Fig. 9. The abrupt nature of the transition from coarse grain to fine grain is evident. Figure 10b shows an EBSD map of this transition region and reveals that, in concert with the change in grain size, the characteristic texture changes from the ⟨001⟩ free-growth

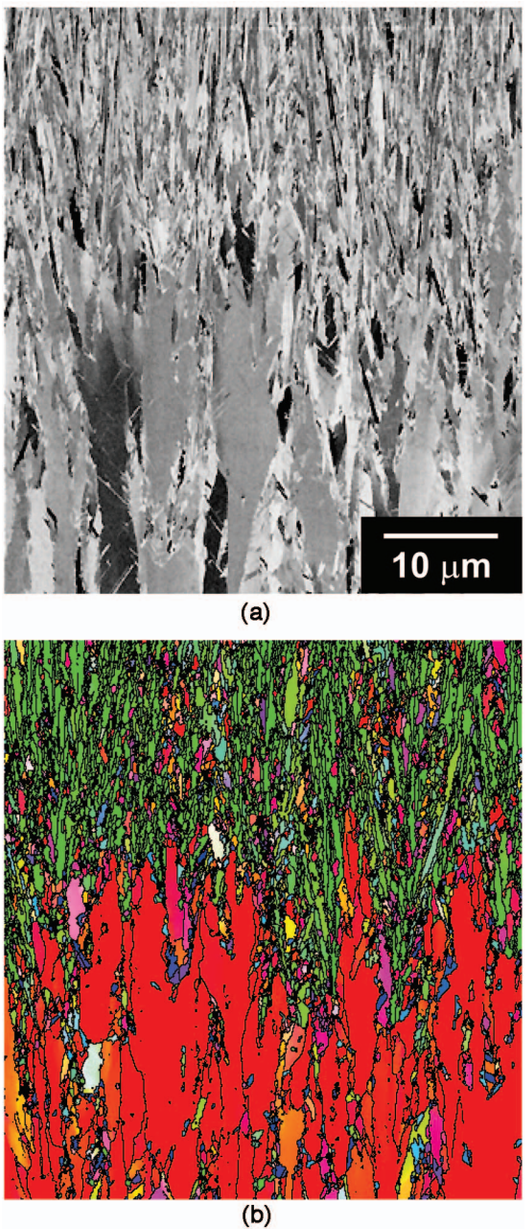

Figure 10. (Color) (a) Higher magnification micrograph of region outlined in Fig. 9. The abrupt change in grain size is apparent and occurs over about a
10-μm region of deposit growth. (b) EBSD map indicates that the texture changes from ⟨001⟩ to ⟨011⟩, indicating that the growth mode changes from uninhibited to inhibited during the deposition run.

texture to the ⟨011⟩ texture characteristic of inhibited growth. XRD-derived texture of planview sections indicate that the ⟨001⟩ free-growth region of the deposit was highly textured (27 times random) and the ⟨011⟩ inhibited-growth region was less strongly, but still significantly, textured (6 times random).

It seems evident, therefore, that the plating parameters established for fabricating this set of specimens result in unstable deposition conditions, allowing the deposit to switch abruptly from coarse-grain, highly ⟨001⟩-textured, uninhibited, free growth to a fine-grain ⟨011⟩-textured, fully inhibited growth mode. Figure 10 shows that the transition from one growth mode to the other occurs over a narrow region of about 10 μm, and faradaic considerations indicate that for the 3 mA/cm^2 current density, the switch in growth modes occurs in approximately 2 h out of a total plating time of roughly 3 days. Sudden changes in film structure, sometimes periodic, that result in nonuniform films or laminate-like films have been previously observed in cross-sectional micrographs of electrodeposited Ni.[9] The behavior in Fig. 10 demonstrates that, under certain conditions, the microstructure of electroplated Ni may quickly change during the deposition, resulting in a nonuniform through-thickness microstructure. This is presumably due to a change in the nature or type of adsorbed species at the solid–liquid interface, such as hydrogen and hydroxides (see below), electrolyte aging species, or species from other chemical reactions occurring in the bulk electrolyte, all of which may result in a change in the film nucleation and growth.

It is clear that in all instances, coarse-grained deposits are associated with the ⟨001⟩ texture indicative of free growth while fine-grained deposits are associated with the characteristic ⟨011⟩ inhibited-growth mode. Rationalizing all of the various observations presented above with respect to growth mode, deposition parameters, and electrolyte condition is difficult. Inhibition during electrodeposition is usually attributed to the presence of an adsorbate, suppressing growth of a certain orientation and promoting the growth of other orientations.[18,20,21] The degree to which such an adsorbate is bound to the growing surface determines, at least to some extent, the temperature and current density regime in which inhibited growth is observed. The insensitivity of the 15 mA/cm^2 deposits with respect to plating conditions can be rationalized in a relatively straightforward manner in that at this higher current density, any inhibiting species that may be present (hydrogen or adsorbed boric acid species, for example) is simply overwhelmed by the high deposition rate. Deposition at this current density, therefore, always occurs in the free-growth mode, regardless of the other plating parameters investigated here (temperature and electrolyte filtration). Similarly, for the electrodeposits plated at 3 mA/cm^2 from filtered electrolyte, deposition is sufficiently slow so as to allow even a weakly bound adsorbate to remain effective in inhibiting growth. Amblard et al. investigated texture evolution in Ni–Watts electrodeposits plated at 50°C and observed a similar transition from fine-grain, ⟨011⟩-oriented (at pH $<$ 2.5) and ⟨112⟩-oriented (pH $>$ 2.5) growth to coarse-grain, ⟨001⟩-oriented growth as current density increased above ~5 mA/cm^2.[20] These authors argued that at lower current density adsorbed hydrogen or $Ni(OH)_2$ inhibited ⟨001⟩ growth while stabilizing ⟨001⟩ and ⟨112⟩ orientations, leading to deposits with these textures. In the present case it is unclear why particle filtering should affect the growth mode, since no change in pH near the cathode upon filtering the electrolyte was observed in Part I of this work.

It is difficult to postulate a single mechanism that can account for the structure and texture of the deposits plated from the unfiltered electrolyte at 3 mA/cm^2. At the lowest deposition temperature, the coarse-grain ⟨001⟩ texture observed in the 3 mA/cm^2 deposit from the unfiltered electrolyte implies free growth and the absence of any inhibiting species, much like both of the deposits plated at the same temperature but at the higher current density. However, compared to the companion deposit from the filtered electrolyte at 28°C and 3 mA/cm^2, it is apparent that the deposition conditions at the metal/electrolyte interface are directly related to the presence or absence of particle filtration in a way that is not obvious. It appears that particle filtration of the sulfamate/boric acid electrolyte promotes the formation of a species that effectively inhibits deposition. Absent the filtration at this temperature and current density, uninhibited growth is the preferred mode.

Most problematic, though, is rationalizing the character of the 50°C, 3-mA/cm^2 deposit from the unfiltered electrolyte. The fine-grain microstructure and ⟨011⟩ preferred orientation of this deposit suggests the presence of an effective adsorbed inhibiting species at the higher temperature that is not present at the lower temperature. Lin et al., who investigated effects of increased ammonium ion con-

centration on sulfamate Ni deposits, also observed a similar trend in texture and microstructure as bath temperature was increased from 40 to 50°C.[22] It is not evident why higher deposition temperatures would lead to increased inhibition at low current densities. One is left, then, with postulating the presence of a second, additional mechanism, perhaps the increased adsorption of a certain sulfamate electrolyte species only at high temperatures and low deposition rates, resulting in inhibited growth under such conditions.

Such a mechanism would help one understand the instability in growth mechanism observed in the 40°C, 3-mA/cm^2 deposit from the unfiltered electrolyte. Given that this temperature is midway between the inhibited and uninhibited growth regimes, this instability would not be surprising, since small perturbations in the growth conditions would translate to major changes in the structure of the deposit.

Conclusions

The structure and properties of nickel deposited from sulfamate electrolytes has been shown to be sensitive to a variety of processing parameters, including current density, deposition temperature, and electrolyte conditioning (particle filtration). The effects are particularly apparent at low applied current density. At 3 mA/cm^2, deposition from filtered electrolyte yields material that is fine-grained and predominantly ⟨011⟩-textured, characteristic of inhibited growth. At 15 mA/cm^2, ED nickel sulfamate deposits are coarse grain and exhibit predominantly ⟨001⟩ texture, characteristic of free or uninhibited film growth irrespective of filtering condition. Low-current-density deposits from unfiltered electrolyte are coarse-grained and ⟨001⟩-textured when plated at 28°C, characteristic of free or uninhibited growth, but are similar in grain morphology and texture to their filtered counterparts when plated at 50°C. At intermediate temperatures, deposits exhibit a dramatic instability in growth mode, growing initially in a free-growth mode but then rapidly transitioning to an inhibited-growth mode.

The mechanical properties of these deposits track with their grain size; the fine-grain deposits resulting from inhibited growth exhibit yield strengths between approximately 750–950 MPa, while larger grain size deposits resulting from uninhibited growth exhibit yield strengths between approximately 350 and 400 MPa.

Acknowledgments

The authors thank Dorrance McLean and John Hachman for their assistance with the fabrication of the test specimens used in this study as well as Andy Gardia, Michael Rye, and Bonnie McKenzie for their assistance with metallographic preparation and microscopy. Sandia is a multiprogram laboratory operated by Sandia Corporation, a Lockheed Martin Company, for the United States Department of Energy under contract DE-AC04-94AL85000.

Sandia National Laboratories assisted in meeting the publication costs of this article.

References

1. D. Baudrand, *Met. Finish.*, **94**(7), 15 (1996).
2. J. L. Marti, *Plating*, **53**(1), 61 (1966).
3. Y. Tsuru, M. Nomura, and F. R. Foulkes, *J. Appl. Electrochem.*, **30**, 231 (2000).
4. Y. Tsuru, M. Nomura, and F. R. Foulkes, *J. Appl. Electrochem.*, **32**, 629 (2002).
5. T. E. Buchheit, D. A. LaVan, J. R. Michael, T. R. Christenson, and S. D. Leith, *Metall. Mater. Trans. A*, **33**, 539 (2002).
6. J. L. Marti and G. P. Lanza, *Plating*, **56**(4), 377 (1969).
7. J. W. Dini and H. R. Johnson, *Surf. Technol.*, **4**, 217 (1976).
8. B. E. Jacobson and J. W. Sliwa, *Plat. Surf. Finish.*, **66**(9), 42 (1979).
9. W. H. Safranek, *The Properties of Electrodeposited Metals and Alloys*, 2nd ed., American Electroplaters and Surface Finishers Society, U.S.A. (1986).
10. J. W. Dini, *Electrodeposition: The Materials Science of Coatings and Substrates*, Noyes Publications, Norwich (1993).
11. A. Ruzzu and B. Matthis, *Microsyst. Technol.*, **8**, 116 (2002).
12. J. W. Dini and H. R. Johnson, *Thin Solid Films*, **54**, 183 (1978).
13. J. I. Goldstein, D. E. Newbury, D. C. Joy, C. E. Lyman, P. Echlin, E. Lifshin, L. C. Sawyer, and J. R. Michael, *Scanning Electron Microscopy and X-Ray Microanalysis*, p. 558, Kluwer Academic/Plenum Publishing, New York (2003).
14. U. F. Kocks, C. N. Tome, and H. R. Wenk, *Texture and Anisotropy, Preferred Orientation in Polycrystals and Their Effect on Materials Properties*, Cambridge University Press, New York (1998).
15. http://eps.berkeley.edu/~Wenk/TexturePage/beartex.html
16. K. J. Hemker and H. Last, *Mater. Sci. Eng., A*, **319-321**, 882 (2001).
17. H. S. Cho, K. J. Hemker, K. Lian, J. Goettert, and G. Dirras, *Sens. Actuators, A*, **103**, 59 (2003).
18. H. Fischer, *Electrodeposition and Surface Treat.*, **1**, 319 (1973).
19. E. O. Hall, *Proc. R. Soc. London*, **64**, 747 (1951).
20. J. Amblard, I. Epelboin, M. Froment, and G. Maurin, *J. Appl. Electrochem.*, **9**, 233 (1979).
21. C. Bergenstof Nielsen, A. Horsewell, and M. J. L. Ostergard, *J. Appl. Electrochem.*, **27**, 839 (1997).
22. C. S. Lin, P. C. Hsu, L. Chang, and C. H. Chen, *J. Appl. Electrochem.*, **31**, 925 (2001).